Supporting Information

Dissolution of Cellulose in Room Temperature Ionic Liquids: Anion Dependence

Rajdeep Singh Payal,[†,‡] Karteek K. Bejagam,[†,‡] Anirban Mondal,[†] and Sundaram Balasubramanian[∗,†]

Chemistry and Physics of Materials Unit

Jawaharlal Nehru Centre for Advanced Scientific Research, Bangalore 560 064, India

E-mail: bala@jncasr.ac.in

[∗]To whom correspondence should be addressed
[†]Chemistry and Physics of Materials Unit
Jawaharlal Nehru Centre for Advanced Scientific Research, Bangalore 560 064, India
[‡]Contributed equally to this work

Table T1 presents characteristics of cellobiose-ionic liquid hydrogen bonding. A strong hydrogen bond is defined as one where the Donor-Hydrogen-Acceptor angle is greater than 150° and the Hydrogen-Acceptor distance is less than 2.5 Å. Weak hydrogen bonds have Donor-Hydrogen-Acceptor angles to be less than 150° and Hydrogen-Acceptor distances less than 2.5 Å. Hydrogen bonds within cellobiose are called intra-molecular, whereas between cellobiose and ILs are termed as inter-molecular.

Table T1: Inter- and intra-molecular hydrogen bonds of cellobiose in gas phase and in ionic liquid media.

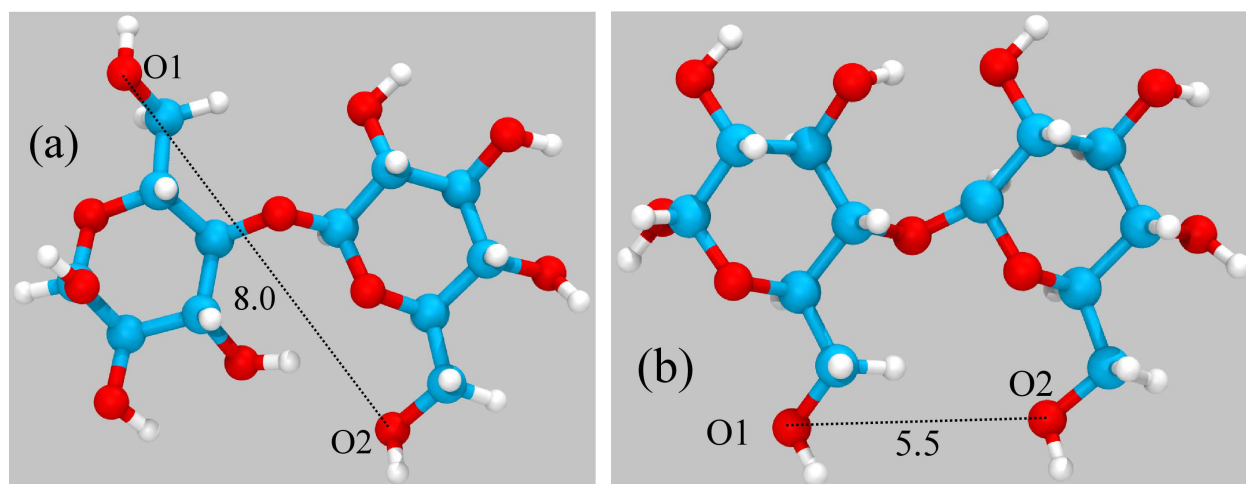| Medium	ϕ (^{o})	Number of strong intra-molecular H-bonds	Number of weak intra-molecular H-bonds	Number of inter-molecular H-bonds
	-165.0	1	2	0
	-115.0	0	2	0
	-75.0	1	2	0
Gas phase	-20.0	3	0	0
	40.0	0	2	0
	100.0	0	2	0
	160.0	2	2	0
	-160.0	2	0	4
	-120.0	1	0	5
	-30.0	1	0	6
[OAc]	15.0	2	0	5
	45.0	0	1	5
	100.0	0	1	5
	145.0	1	1	5

Figure S1: (a) Anti-anti and (b) anti-syn conformers of cellobiose. Color scheme C: Cyan, O: Red and H: Blue. Distance (in Å) between hydroxyl oxygens atoms (O1, O2) in the two hexose rings marked. The same can be used to distinguish the two conformational states.
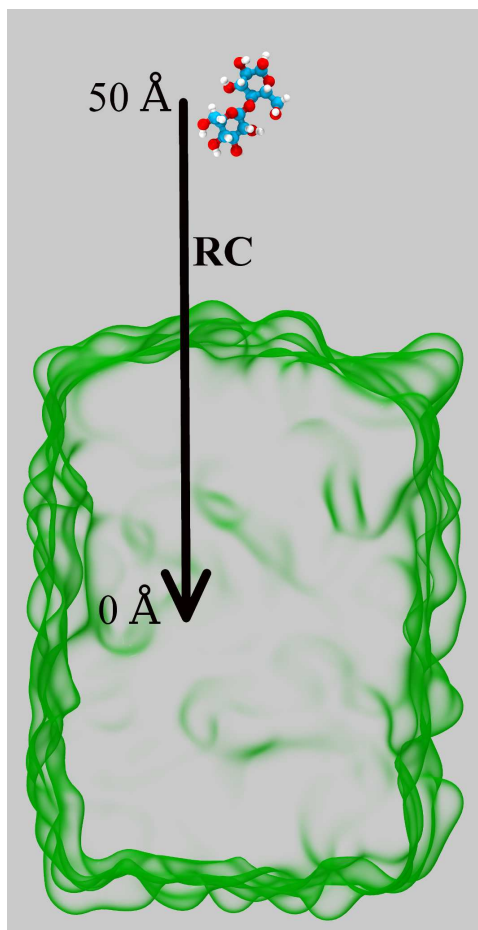
Figure S2: Reaction coordinate for solvation free enegry calculation of cellobiose in ILs.
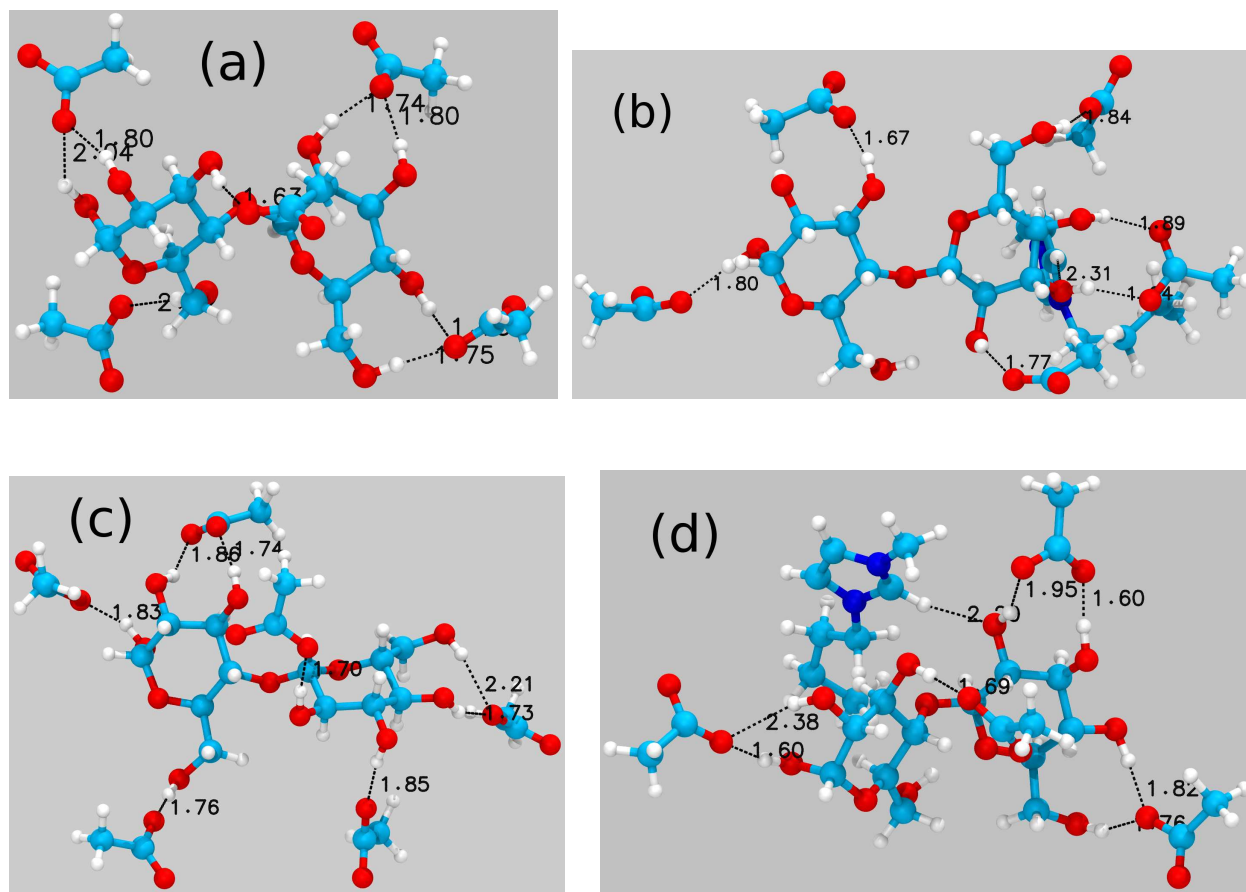
Figure S3: Hydrogen bonded ions around cellobiose in [bmim][OAc] at ϕ values (a) -160°, (b) -45°, (c) 120° and (d) 170°. Color scheme same as previous figures.
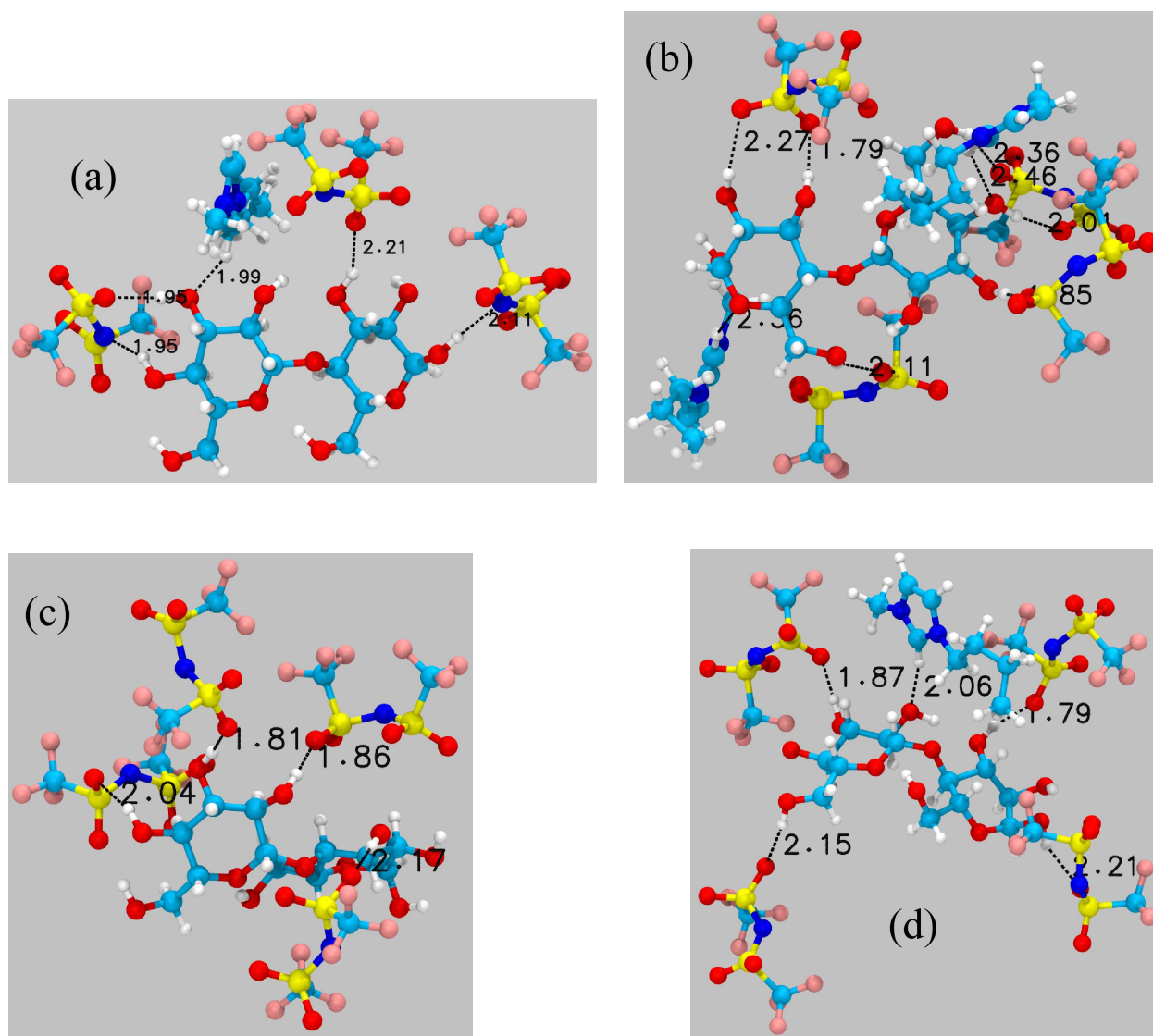
Figure S4: Hydrogen bonded ions around cellobiose in [bmim][NTf$_2$] at ϕ values (a) -160°, (b) -25°, (c) 120° and (d) 170°. Color scheme same as previous figures, S: Yellow and F: Pink.
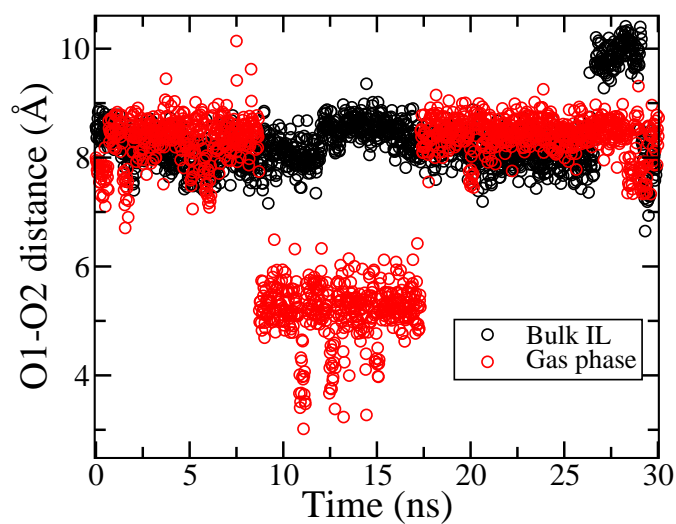
Figure S5: Distance between O1 and O2 atoms of cellobiose in gas phase and in bulk [bmim][OAc] during the solvation free energy simulations. Cellobiose is found to be in the anti-anti conformation in bulk IL and mostly so in the gas phase window. For the definitions of O1 and O2, refer Figure S1.

In Figure 3 (main text) , the SFE profile for all ILs except [bmim][NTf$_2$] and [bmim][Cl] start changing at 38 Å. However, for these two ILs, the SFE profiles exhibit changes at around 40 Å. This observation can be explained by examining the density profile of the ions which is shown in Figure S6(a). The mean density in the bulk liquid region of the profile closely matches the values obtained from bulk-NPT simulations,[1] as expected. Due to the larger molecular volume of [NTf$_2$] anion, the profile for [bmim][NTf$_2$] extends up to 40 Å on either side of the centre of mass. The thicker liquid slab thus leads to a wider SFE profile. Although the liquid-vapor interface of [bmim][Cl] is sharp (in terms of density profiles), its SFE profile at the interface is wide; during the ABF MD simulations, the displacement of a few chloride ions from the liquid phase towards cellobiose (which was in gas phase) was observed. This is the underlying cause for the width in its SFE profile (Figure S7). As an illustrative case, Figure S6(b) shows the number density profile of cation ring center, anion center of mass and butyl terminal carbon atom of cation for [bmim][NTf$_2$]. As with many other ILs,[2] the interface is enriched with the butyl tail which is oriented nearly normal to the interface plane. An ultra-thin dielectric layer exists at the interface wherein the anion is present closer to the vapor phase and the cation lies closer to the liquid phase.
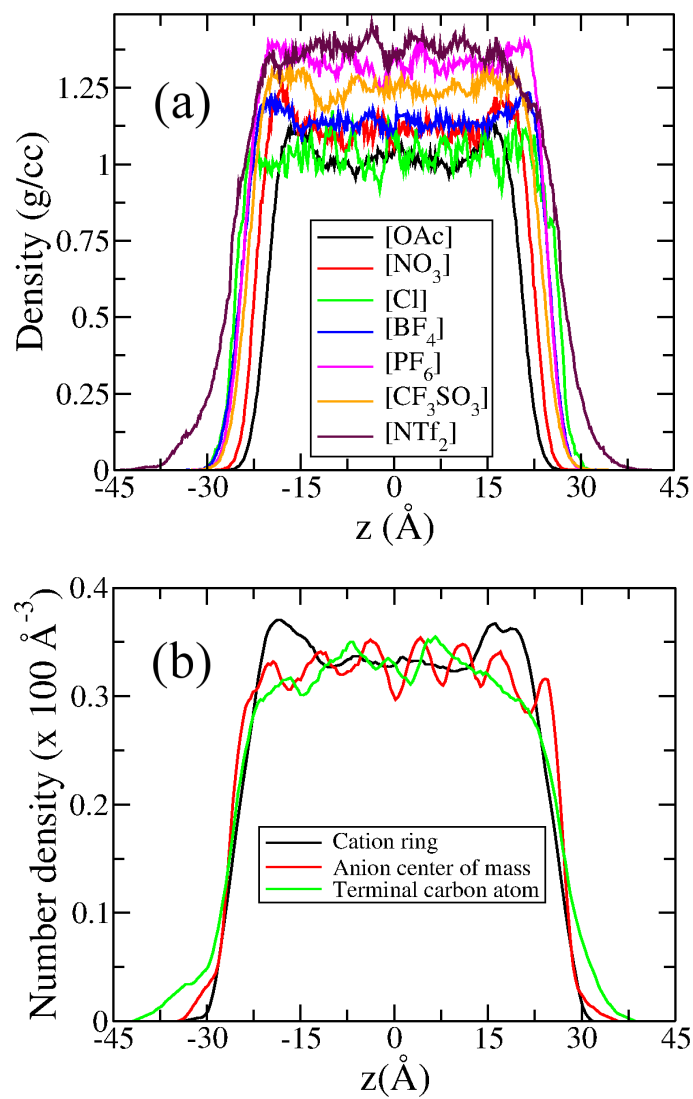
Figure S6: (a) Mass density profile of ionic liquids and (b) number density profile of cation ring center, anion center of mass and terminal carbon atom of butyl tail in [bmim][NTf$_2$]. [bmim] is cation and T= 353 K.
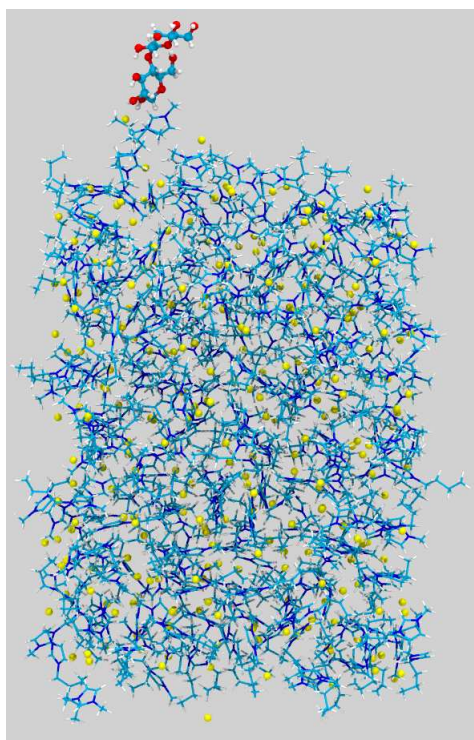
Figure S7: Snapshot of the simulation showing cellobiose present in gas phase disrupting the liquid-vapor interface for [bmim][Cl]. Color scheme Cl: Yellow, O: Red, C: Cyan, N: Blue and H: White.

Binding energy calculations: Firstly, an ion pair of IL and cellobiose were geometry optimized independently under isolated conditions. Later, that ion pair was placed at different (around ten) locations around cellobiose and geometry optimizations were initiated from each such configuration using the emprical force field. Binding energy of cellobiose with the ion pair was determined in each of these runs and the best one is reported in Table T2.

Table T2: Binding energy of cellobiose with ion pair where [bmim] is the cation, compared against its solvation free energy in the bulk ionic liquid.

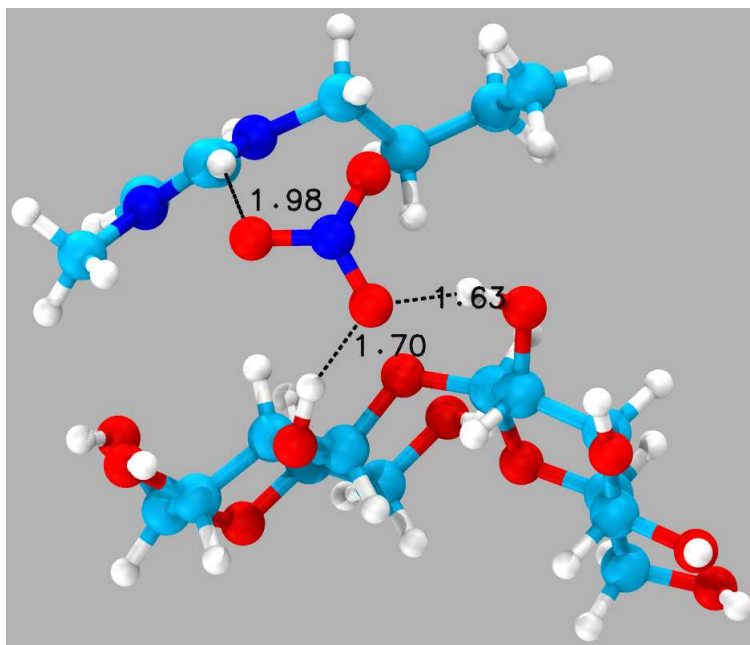| IL	Binding Energy (kcal/mol)	Solvation free energy (kcal/mol)
[OAc]	-31.8	-56.4
[NO$_3$]	-31.4	-53.7
[Cl]	-29.7	-49.9
[BF$_4$]	-25.6	-41.7
[PF$_6$]	-26.8	-36.5
[CF$_3$SO$_3$]	-26.0	-38.2
[NTf$_2$]	-27.9	-38.8

Figure S8: Geometry optimized, minimum energy configuration for cellobiose and [bmim][NO₃], obtained via force field calculations in gas phase. Important intermolecular distances (in Å) are displayed.
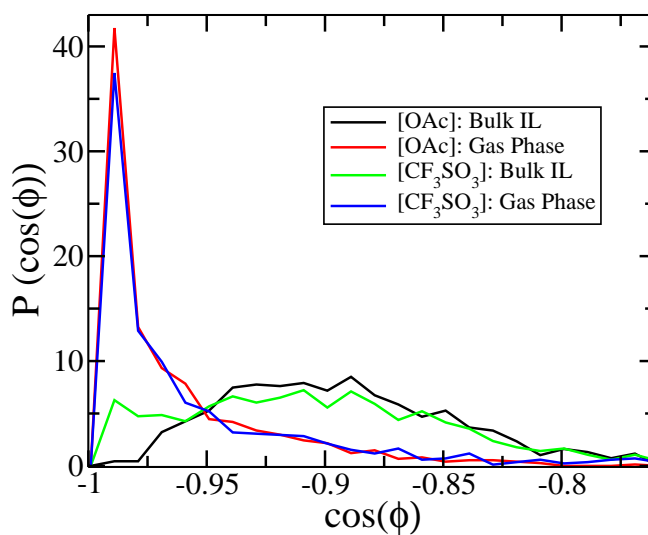

Figure S9: Distribution of angle between ring normals of cellobiose in gas phase and bulk IL.

References

(1) Mondal, A.; Balasubramanian, S. Quantitative Prediction of Physical Properties of Imidazolium Based Room Temperature Ionic Liquids through Determination of Condensed Phase Site Charges: A Refined Force Field. *J. Phys. Chem. B* **2014**, *118*, 3409–3422.

(2) Bhargava, B.; Balasubramanian, S. Layering at an Ionic Liquid-Vapor Interface: A Molecular Dynamics Simulation Study of [bmim][PF$_6$]. *J. Am. Chem. Soc.* **2006**, *128*, 10073–10078.